



## Research article

# Modelling particulate matter (PM2.5) source contributions for air pollution management in Addis Ababa, Ethiopia

Sarath K. Guttikunda <sup>a,b,\*</sup>, Sai Krishna Dammalapati <sup>b</sup>, Worku Tefera <sup>c,1</sup>, Jian Xie <sup>d</sup>

<sup>a</sup> TRIP Centre, Indian Institute of Technology, New Delhi, India

<sup>b</sup> Urban Emissions Information, Goa, India

<sup>c</sup> Unity Healthcare Inc., Washington, DC, USA

<sup>d</sup> The World Bank, Washington DC, USA

## ARTICLE INFO

## Keywords:

Addis Ababa  
Ethiopia  
Air quality  
PM<sub>2.5</sub>  
Ambient monitoring  
Urban air quality management  
WRF-CAMx  
Source apportionment  
Emissions inventory

## ABSTRACT

Ground measurements and satellite observations over Addis Ababa airshed show a deteriorating trend of air pollution, especially for PM<sub>2.5</sub> (all particulate matter under 2.5  $\mu\text{m}$ ). In this paper, we present a review of available monitoring data; a model-ready multi-pollutant (PM<sub>10</sub>, PM<sub>2.5</sub>, SO<sub>2</sub>, NO<sub>x</sub>, CO, non-methane VOCs, and CO<sub>2</sub>) emissions inventory at 0.01° resolution for the designated airshed; a heatmap of PM<sub>2.5</sub> concentrations and an estimate of source contributions constructed using WRF-CAMx chemical transport modelling system; and a discussion on proposed actions towards establishing an air quality management plan for the city. Emissions from road transport; residential and commercial cooking; resuspended dust on roads and from construction activities; residential and industrial heating; open waste burning; and other industrial activities contributed to annual average ambient PM<sub>2.5</sub> pollution levels ranging 20–60  $\mu\text{g}/\text{m}^3$ . Particularly, vehicle exhaust is estimated to contribute up to 29 % of total PM<sub>2.5</sub>, followed by biomass combustion in the residential and industrial sectors.

## 1. Introduction

A successful urban air quality management (AQM) plan begins by comprehending the sources of air pollution, identifying opportunities to reduce emissions, and prioritizing local and regional initiatives aimed at enhancing air quality [1–4]. For example, in areas with high levels of vehicle emissions, efforts can focus on promoting alternate transport modes such as public transit, carpooling, and cycling; in areas with heavy industrial pollution and substantial contributions from biomass use for cooking and heating, efforts can focus on promoting efficient technologies and cleaner fuels. An informed AQM plan with baseline information on emission sources, emission inventories, pollution heatmaps, and a network of monitoring stations, lays a strong foundation for cost-benefit analysis of emission control options and public-policy dialogues. Efforts to develop these knowledge baselines and analytical methodologies for AQM are limited and at the nascent stage in the low- and middle-income countries, especially among the African cities [5].

Ethiopia has experienced a 10 % annual urbanization rate since 2008 and is projected to have 40 % of its population living in urban areas by 2050. Despite economic progress, air pollution remains the second leading risk factor for premature death [6]; [7–10]. Between 1998 and 2021, Ethiopia's annual average PM<sub>2.5</sub> concentrations increased by 30–40 %, based on global reanalysis combining

\* Corresponding author. TRIP Centre, Indian Institute of Technology, New Delhi, India.

E-mail address: [sguttikunda@gmail.com](mailto:sguttikunda@gmail.com) (S.K. Guttikunda).

<sup>1</sup> (formerly, School of Public Health, Addis Ababa University, Addis Ababa, Ethiopia).

satellite data, ground measurements, emission inventories, and chemical transport models [11]. Between 1990 and 2021, annual premature deaths in Ethiopia due to PM2.5 exposure shifted from 109,000 (ranked 2nd) to 76,000 (ranked 1st), including both indoor and outdoor pollution. In Addis Ababa, ambient air pollution alone causes an estimated 2,000 premature deaths annually. The rise in commercial, economic, and industrial activities in cities like Addis Ababa is driving increased energy and transport demand, leading to higher air pollution levels [5,12–15]. An analysis of visibility data in Addis Ababa shows a declining trend since the 1970s, raising growing concerns [16].

Quantification of contribution of sources inside and outside a city is accomplished using sampling and chemical analysis-based receptor models and using emission inventory-based chemical transport models. For this study, we utilized the latter approach. In this paper, we present an analysis of the current state of air quality in Addis Ababa, including (a) a review of available monitoring data, (b) a multi-pollutant emissions inventory, (c) a heatmap of PM<sub>2.5</sub> concentrations and source contributions constructed using a chemical transport modelling system and validated against ground monitoring data, and (d) a list of proposed actions towards establishing an AQM in the city. The multi-pollutant emissions inventory in model-ready gridded (0.01°) format for the designated airshed is included in the supplementary, along with a copy of the results from the WRF-CAMx simulations for PM<sub>2.5</sub> concentrations and source apportionment. For the Addis Ababa region, this is the first open-access high resolution emissions inventory and pollution modeling attempt in the published literature.

## 2. DATA and METHODS

The multi-pollutant emissions inventory includes the following: particulate matter (PM) in two size fractions – everything under 2.5 μm (PM<sub>2.5</sub>) and everything under 10 μm (PM<sub>10</sub>); black carbon (BC); organic carbon (OC); sulfur dioxide (SO<sub>2</sub>); nitrogen oxides (NOx) – combination of nitrogen dioxide (NO<sub>2</sub>) and nitric oxide (NO); carbon monoxide (CO); and volatile organic compounds (VOC). The target pollutant and metric for chemical transport modeling and policy discussions in this paper is total PM<sub>2.5</sub> concentrations.

Other most used abbreviations in this paper are the following: air quality management (AQM); carbon dioxide (CO<sub>2</sub>); Comprehensive Air Quality Model with Extensions (CAMx); Federal Transport Authority (FTA); greater Addis Ababa Airshed region (GAAR); greenhouse gas (GHG); geospatial information systems (GIS); Weather Research Forecasting (WRF) model.

**Table 1**

Publications and online data repositories accessed to establish necessary activity information for energy and emissions analysis and the models utilized for pollution analysis (all links were last accessed on June 26th, 2024).

Category	Resource
Publications	<p>1 Addis Ababa 2016 Greenhouse Gas Emissions Inventory Report, by the C40 Cities program (London, UK)</p> <p>2 Urban Air Quality Management in Ethiopia: A Guidance Framework, by Center for Science and Environment (New Delhi, India)</p> <p>3 Motorization management in Ethiopia, by The World Bank (Washington DC, USA)</p> <p>4 Addis Ababa City Air Quality Management Plan, by Addis Ababa Environmental Protection and Green Development Commission, with support from the US EPA, the United States Embassy in Addis Ababa, and UN Environment Program (UNEP).</p>
Monitoring data	<p>5 AirNow program operating ambient monitors at the US Embassy locations in the city (<a href="https://www.airnow.gov/international/us-embassies-and-consulates">https://www.airnow.gov/international/us-embassies-and-consulates</a>)</p> <p>6 AddisAir low-cost sensor network (<a href="https://airquality.addisababa.info">https://airquality.addisababa.info</a>)</p>
Statistics	<p>7 EthioInfo dashboard of the Statistical Office of Ethiopia (<a href="http://www.dataforalldemo.org/dashboard/v1/ethioinfo/ethioinfo#/">http://www.dataforalldemo.org/dashboard/v1/ethioinfo/ethioinfo#/</a>)</p> <p>8 Federal Transport Authority (FTA) Ethiopia via staff communications</p>
Open access databases	<p>9 STATISTA online commercial data repository (<a href="https://www.statista.com">https://www.statista.com</a>)</p> <p>10 Open Street Maps (OSM) database (<a href="https://www.openstreetmap.org">https://www.openstreetmap.org</a>)</p> <p>11 Global human settlements (GHS) program for urban-rural classification (<a href="https://ghsl.jrc.ec.europa.eu/datasets.php">https://ghsl.jrc.ec.europa.eu/datasets.php</a>)</p> <p>12 LANDSCAN program for gridded population (<a href="https://landscan.ornl.gov">https://landscan.ornl.gov</a>)</p> <p>13 FlightStats (<a href="https://www.flightradar24.com">https://www.flightradar24.com</a>)</p> <p>14 Google Earth application for image scanning for points of interests like industrial estates and quarries (<a href="https://earth.google.com">https://earth.google.com</a>)</p> <p>15 Google Earth Engine platform, to access two satellite products, ultraviolet aerosol index (UVAI) from TROPOMI and aerosol optical depth (AOD) from MODIS-MAIAC, to correlate trends in particulate pollution and energy consumption in the region. (<a href="https://developers.google.com/earth-engine/datasets">https://developers.google.com/earth-engine/datasets</a>)</p>
Models	<p>16 Pollution modeling was conducted using the CAMx (<a href="https://camx.com">https://camx.com</a>), an Eulerian photochemical transport model, which supports advection, scavenging (dry and wet deposition), chemical solvers for multiple chemical mechanisms including conversion of gases to aerosols, such as SO<sub>2</sub> to sulfates, NO<sub>x</sub> to nitrates, and VOCs to secondary organic aerosols; and plume rise calculations for point sources using 3-dimensional meteorological data. The CAMx modeling system is open-source, modular, and supports source apportionment calculations. The boundary conditions for the airshed were obtained from the MOZART/CAMchem global system (<a href="https://www2.acom.ucar.edu/gcm/cam-chem">https://www2.acom.ucar.edu/gcm/cam-chem</a>), for which a pre-processing module is available, along with other useful tools for post-processing of the model results. The model results were compared against all the available ambient air quality data to evaluate the emission inventory qualitatively and quantitatively.</p> <p>17 The meteorological data was extracted from WRF modeling system (<a href="https://github.com/wrf-model/WRF">https://github.com/wrf-model/WRF</a>) at the spatial and temporal resolution necessary for the CAMx model simulations. A summary excel file for the airshed is included in the supplementary and the model-formatted files are available upon request via email. Global input fields for the model are available from NCEP's Global Data Assimilation System (GDAS - <a href="https://www.ncei.noaa.gov/products/weather-climate-models/global-data-assimilation">https://www.ncei.noaa.gov/products/weather-climate-models/global-data-assimilation</a>). This data is available at multiple spatial resolutions – 1.0°, 0.5° and 0.25° to suit regional and urban scale downscaling exercises.</p>

## 2.1. Data resources

All the activity data necessary for emissions analysis is collated from the best available open resources including census information, satellite feeds, open GIS datasets, and published literature. No primary surveys were conducted for this study, such as surveys for in-use vehicle characteristics [17] or surveys for fuel consumption at the household level [18]. Published literature and supporting online databases used to collate necessary information on energy consumption and sectoral activities are listed in Table 1. A copy of the documents and data extracted (in standard GIS format) is included in the supplementary. These studies and databases were used to establish activity information necessary for building an operational emissions inventory, such as household energy consumption, vehicle stock and usage numbers, waste management, and overall air quality.

## 2.2. Designated airshed region

For the Greater Addis Ababa Region (GAAR), the designated airshed spans between 38.5°E to 39.1°E in longitude and 8.7°N to 9.2°N in latitude, at a grid resolution of 0.01°. This area covers the main city, satellite cities, industrial estates, landfill, and quarries (Fig. 1a). This extended airshed allows for estimating the source contributions from inside and outside the city boundaries. The purple lines represent the ten districts (1) Akaki Kality in the southeast is known for its industrial areas and large low-income residential developments (2) Arada is the central commercial district (3) Bole is the city's fastest-growing district, with a high concentration of modern residential developments and shopping centers (4) Gulele in the west of the city hosts most of the embassies (5) Kirkos in the north is known for its universities (6–7) Kolfe Keranio in the southwest and Mekanisa in the northwest are known for hosting government offices and diplomatic missions (8) Nefas Silk in the west of the city is a new development (9–10) Yeka in the east and Sengatera in the south are the old towns.

The black lines in Fig. 1a represent 1350 km of primary roads (including highways), and grey lines are 17,600 km of all mapped roads (from OSM database) in the airshed. The road density (km/grid) information is segregated into highways, arterial roads,

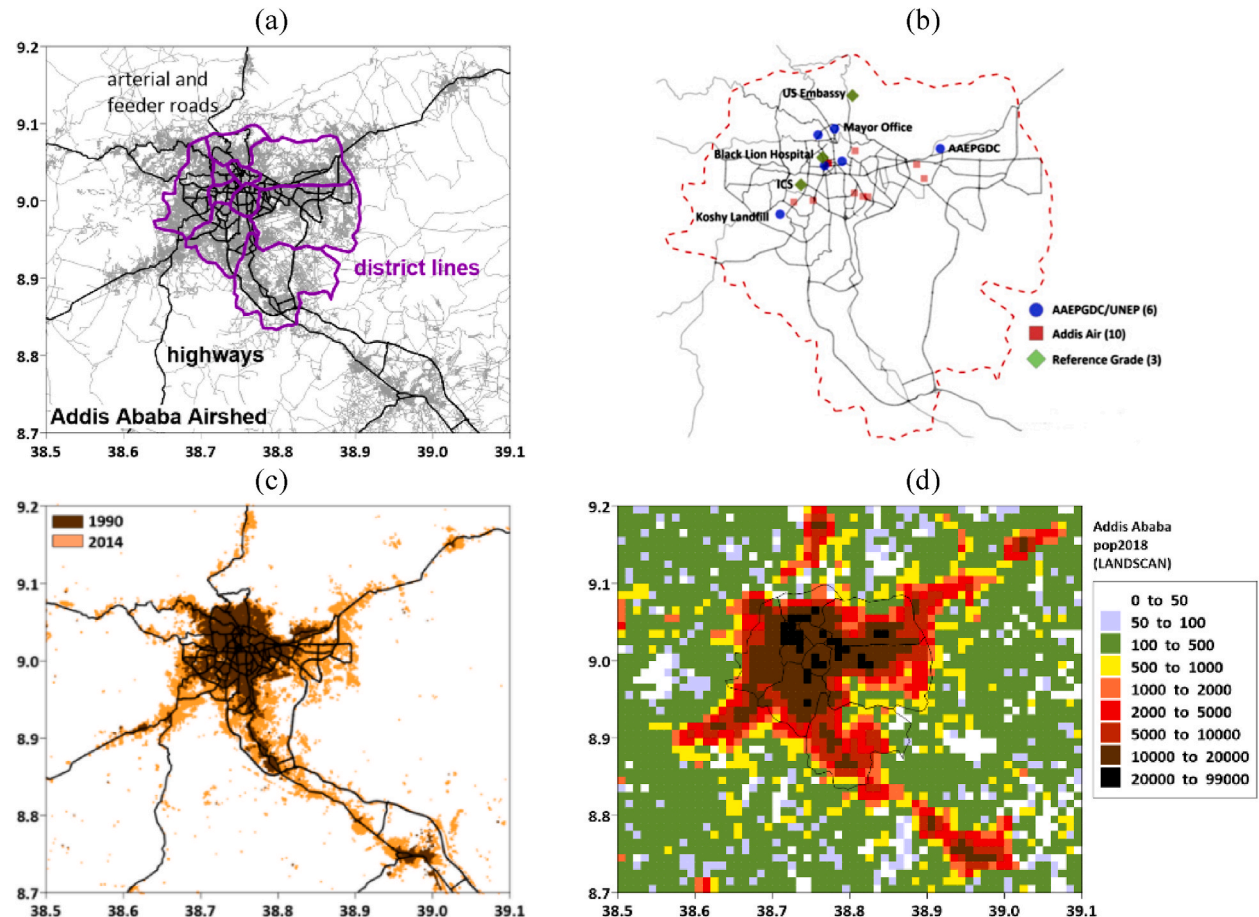


**Fig. 1.** (a) Extent of the greater Addis Ababa airshed covering the main city province and the neighborhood with potential to directly influence the urban air quality (b) location of the ambient air monitoring stations (c) urban built-up area for 1990 and 2014 from ESA's Global Human Settlements program and (d) gridded population density from the LANDSCAN program.

secondary roads, and feeder roads, and is a representation of the personal and freight movement corridors. A total of 11,430 commercial activity points were extracted from OSM database, including apartment complexes, banks, cafes, commercial complexes, fuel stations, hotels, hospitals, industries, malls, markets, office complexes, parking lots, restaurants, and shops. These layers were used as spatial proxies for emissions distribution from heavy-duty vehicles (mainly on highways) and passenger cars (across city roads), with commercial activity density serving as variable grid weights where vehicles idle for pickups and drop-offs. The assumption is that the vehicle kilometers traveled in each grid are proportional to the road length mapped within it.

The brown and orange shades in [Fig. 1c](#) represent the built-up area information for 1990 and 2014, which increased 190 % with 18 % of the GAAR designated as urban. The built-up area and the road network density coincides with the higher population density grids ([Fig. 1d](#)). Most of the area outside the urban grids is designated for agriculture and vegetation. In 2018, the airshed population was 4.9 million, projected to reach 6.6 million by 2030. The urban-rural population split was 87-13 % in 2018 and is expected to be 88-12 % in 2030. This limited change is due to the absence of major plans to expand city limits or relocate urban populations. In 2018, 56 out of 3,000 grids had a population density exceeding 30,000 per square kilometer. This gridded population data is used to estimate total emissions and spatially disaggregate emissions across multiple sectors. For instance, population density and household size are key inputs for estimating the energy required by each grid for residential activities. Population density also serves as an initial proxy for commercial and transport activity, further refined by data on road and commercial activity density to map vehicle exhaust emissions.

### 2.3. Ambient air quality data

Since 2014, the National Meteorological Administration has operated three ambient monitoring stations. The USEPA's AirNow International program runs two Beta Attenuation Monitoring (BAM) stations at the US Embassy—one in Central Addis since 2016 and another in Jacros since 2020. The monitoring network in GAAR has gradually expanded to include both reference-grade and low-cost sensor stations ([Fig. 1b](#)). While the initial phase of low-cost sensors faced power and internet connectivity issues, they ultimately enhanced the spatial coverage of the ambient monitoring network.

### 2.4. Activity data for emissions inventory

The emissions inventory was established using activity-based methodology modified for different sources. The approach involves identifying all activities that result in emissions and disaggregating the emissions into the model grids using spatial proxies. This is a globally accepted and applied approach at urban, national, and regional scales for analyzing emissions and pollution, conducting cost-benefit analysis of scenarios, and evaluating health impacts [2,3,8,19,20]. The methodology for putting together the activity data, the equations for calculating the emissions, and the methodology for spatial disaggregation of the emissions are documented in Refs. [4]; [21,22]. Representative sector average emission factors are extracted from regional models [20,23]. A detailed database of these factors are included in Refs. [24]. In addition to accessing the resources listed in the data section, Google Earth Imagery was used for identifying the sources not immediately available for scrutiny. A composite presentation with a summary of the emissions sources identified and supporting information is included in the supplementary. A library tools for emission calculations and for capacity building are available at <https://urbanemissions.info/tools>.

Vehicle fleet information by type and by age was collated from FTA Ethiopia. The raw list includes 25 vehicle types ranging from 2-wheelers to trailers. These 25 categories were clubbed into 11 broad vehicle categories ([Table 2](#)) for the ease of overall emission calculations. Ethiopia's total registered vehicle fleet size in 2020 was 1.2 million, with approximately 50 % registered in Addis Ababa [25]. Geographically, the central location of Addis Ababa allows for regular inter-regional transport of vehicles registered in the regions of Afar, Amhara, and Oromia. Overall, the city vehicle fleet is dominated by 4-wheelers, followed by freight vehicles and buses. The 2- and 3-wheelers are limited in the current fleet but are expected to increase in the future fleet. The modal share of passenger km-traveled is split between motorized and non-motorized transport – with walking and cycling at 46 %, public transport using mini-buses at 45 % and private vehicles at 9 %. In the transport sector, volume of diesel sales is 6–7 times the petrol sales, with most of the consumption by all the buses. Information on vehicle usage characteristics and vehicles split by fuel is extracted from the reports from C40 cities program and the World Bank ([Table 1](#)) [24]. The second-hand vehicle sales market is strong in the region, and it is reflected in the age mix of the vehicles. A large portion of diesel buses and more than 50 % of the passenger vehicles are older than 10 years [26]. Older vehicles, irrespective of the inspection and maintenance programs in the city, are known to observe higher emission rates and lower fuel efficiency in Addis Ababa and other cities [27]; [28].

According to the international Energy Agency outlook for Ethiopia, while only 50 % of the population has access to electricity, nearly 100 % of the electricity generation is met via renewables in the form of hydro and biomass-based power. The residential cooking and heating demand and industrial energy needs are met using the abundant biomass resources (~88 %), followed by oil combustion in the transport sector (~9 %) and the rest via renewables [29]; [30]. Total estimated biomass consumption in Addis Ababa in the form of wood, crop residue, saw dust, and dung is approximately 2.5 million tons, supporting the energy demand of approximately 10–14 GJ/household/year [31]. This demand is higher in the rural areas, especially for heating needs, with limited access to alternative fuels. The urban-rural classification from the GHS program was overlayed with the gridded population and gridded 2m-temperature profiles to estimate the energy demand and emissions at the grid level. The temperature profile provides seasonality information in modulating the total emissions over a year.

Google Earth platform was utilized for visual information on sources across the airshed, which was later used to correlate with the existing databases. This process also led to an understanding of the landscape of the region. For example, [Fig. 2](#) presents a summary of mapped industrial estates from manual scanning of the airshed grids. The scanning process is designed to identify all known industrial

**Table 2**

Number of registered vehicles in Ethiopia in 2020 by clubbed category and region (AA = Addis Ababa; AM = Amhara; AF = Afar; BN = Benishangul; DD = Dere Dawa; SO = Somali; TG = Tigari; GM = Gambela; HA = Harari; SN = South People; OR = Oromiya; 2Ws = 2-wheelers; 3Ws = 3-wheelers; MUVs = multi-utility passenger vehicles; BUS1 = small buses; BUS2 = big buses; HDV = heavy duty vehicles; LDV = light duty vehicles).

Description	AA	AM	AF	BN	DD	SO	TG	GM	HA	SN	OR	Total
2Ws	25,726	45,137	1,355	6,108	7,656	1,651	14,405	2,370	1,076	76,565	61,386	243,435
3Ws	372	19,661	3,925	2,662	3,095	8,773	18,521	0	4,909	11,325	55,466	128,709
Cars	218,229	1,750	81	52	2,313	635	1,954	316	1,277	96	5,153	231,856
MUVs	96,407	5,785	896	534	2,040	2,138	3,660	323	353	1,870	6,237	120,243
Taxis	6,421	154	20	12	89	57	115	13	33	40	232	7,186
BUS1	28,432	9,197	493	375	1,656	979	5,656	2,125	80	13,300	27,315	89,608
BUS2	17,707	13,953	678	467	786	871	4,473	859	3,000	9,617	32,289	84,700
HDV	125,898	3,980	296	110	4,763	2,790	5,806	0	0	3,679	7,677	154,999
LDV	44,898	3,597	338	105	1,041	1,104	1,298	0	0	1,577	1,839	55,797
Offroad	34,774	817	69	143	530	10	3,885	0	0	17	986	41,231
Others	31,576	2,403	126	87	541	571	1,027	231	0	338	5,446	42,346
Total	630,440	106,434	8,277	10,655	24,510	19,579	60,800	6,237	10,728	118,424	204,026	1,200,110

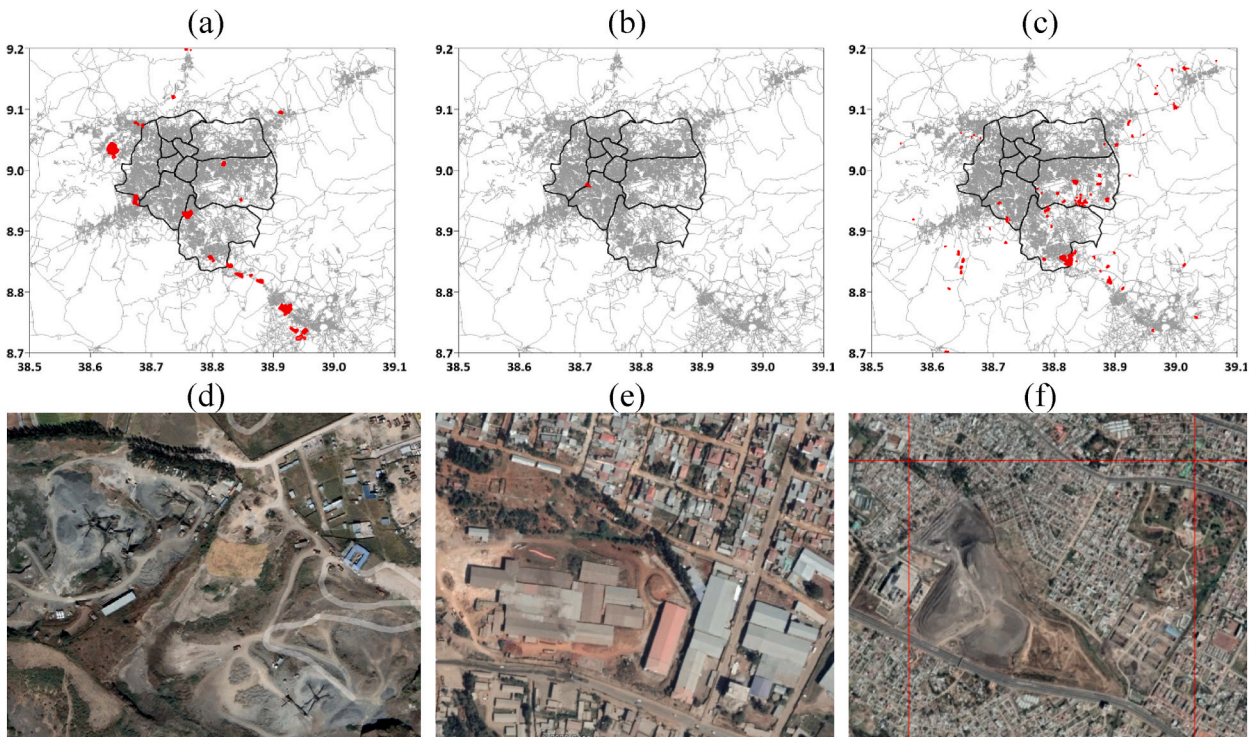


**Fig. 2.** (a) Mapped industrial areas (b) Mapped landfill area (c) mapped rock quarries. Images sourced from the Google Earth platform (d) an example rock quarry (e) brick kiln (f) repi landfill.

structures like a cement factory, a cluster of small industrial units (Fig. 2a) and quarries (Fig. 2c-d), brick kilns (Fig. 2e), and a landfill (Fig. 2b-f). The Mugar cement plant, established in 1983, is located 10 km from Addis's western administrative boundary with an installed capacity to produce 1.5 million tons of clinker and 2.3 million tons of cement per year [32]; [33]. In Addis, approximately 30 % of waste is reported uncollected, with an open waste burn rate of 30 % and 50 % of the uncollected waste in the urban and rural areas respectively [34]; [35]. The landfill, commonly known as "repi" covers an area of 0.5 km<sup>2</sup> and has a collection and processing capacity of 2,000 tons per day (Fig. 2b). Instances of quarries are presented in Fig. 2c, which represent a total area of 9 km<sup>2</sup> spread across the airshed. These quarries, during the non-rainy season, are hotspots for dust resuspension from rock crushing and processing activities [36]; [37]. GIS layers of the mapped industrial estates and quarries are included in the supplementary.

### 3. Results and discussion

#### 3.1. Meteorological data

GAAR falls under a subtropical highland climate, with an average elevation of 2,300 m above sea level. The meteorological summary in Fig. 3 is modeled using WRF (version 4.3), incorporating inputs from the National Centers for Environmental Prediction (NOAA/NCEP) at a 0.25° resolution under the Global Data Assimilation System (GDAS) program (Table 1). The model set-up in 15-3-1 km nested mode was parameterized with Kain-Fritsch scheme (option 1) for cumulus physics, Yonsei University scheme (option 1) for boundary layer physics, WRF Single-Moment 6-class scheme (option 6) for microphysics, Rapid Radiative Transfer Model (option 4) for shortwave and longwave radiation and adaptive timesteps. The conversion of WRF outputs to model-ready formats at 0.01° spatial resolution and 1 h temporal resolution was done using CAMx pre-processors. A comparison of WRF output patterns and historical weather patterns is included in a composite presentation in the supplementary.

The model output provides all necessary meteorological fields for chemical transport modeling using CAMx. Prevailing wind direction shifts from westerly during June to August to easterly for the rest of the year, influencing GAAR's energy and emissions patterns. Wind speed remains consistent year-round. Nighttime winter temperatures often drop below 10 °C, sometimes as low as 5 °C, necessitating continuous space heating, primarily from combustion of wood, crop residue, coal, and cow dung. Mixing heights (not shown here), lowest during June to August, increase pollution levels by restricting emission dispersion. On average, nighttime mixing layers are half the height of daytime layers. Despite cold temperatures and rainy summers, the city enjoys sunny, clear weather, making it ideal for outdoor activities. Summary animations of these meteorological features are included in the supplementary material.

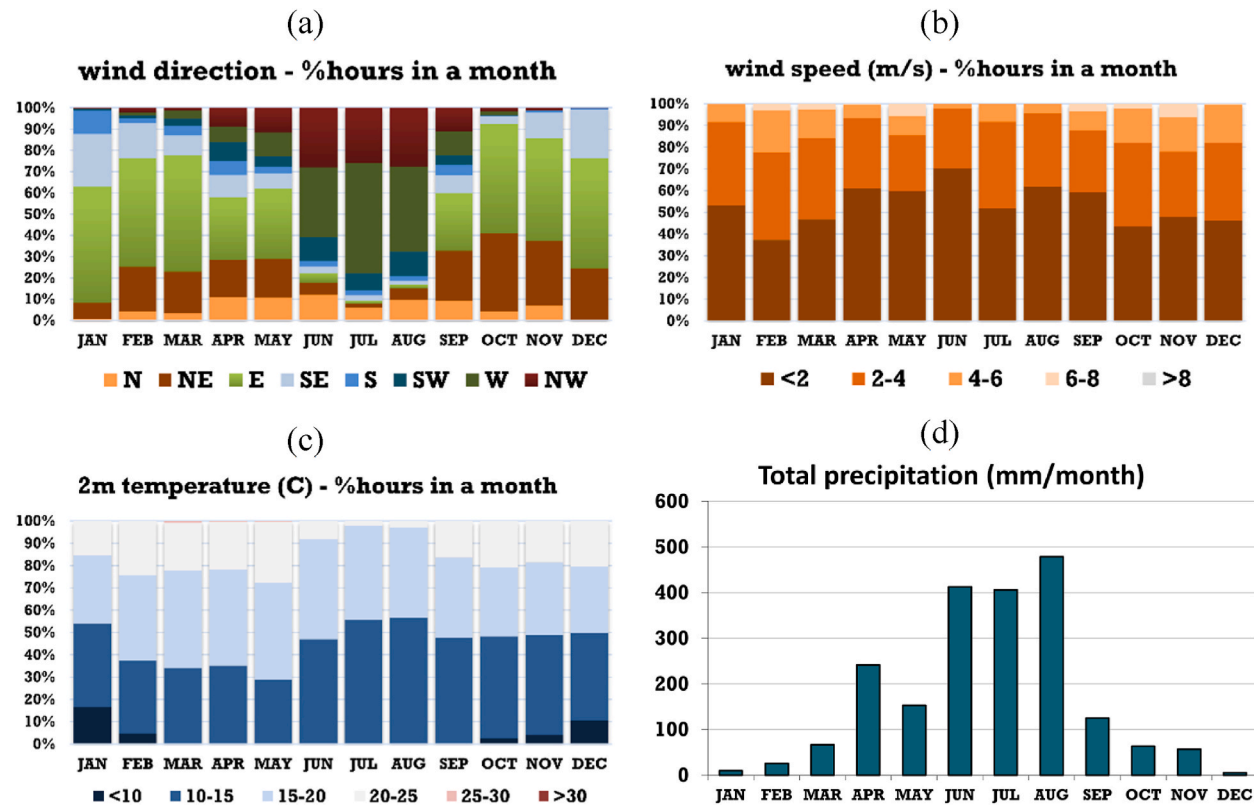


**Fig. 3.** Percent hours in variations bins in each month for (a) wind direction (b) wind speed and (c) 2m-temperature and (d) total precipitation by month, extracted from WRF meteorological modeling system.

### 3.2. Ambient monitoring data and satellite observations

A summary of PM<sub>2.5</sub> concentrations from the two US Embassy stations and all the data from the reference-grade stations and the low-cost sensor network in GAAR is presented in Table 3 and Fig. 4 (orange bars). Six Kunak-cloud sensors were installed by the United Nations Environment Programme (UNEP) and ten sensors were installed by Addis-Air to measure PM<sub>2.5</sub> concentrations using the light-scattering method. Between the BAMs and the low-cost sensors, there is representative spatial coverage for ambient PM<sub>2.5</sub> pollution monitoring.

All the data shows highs during June to August and tapering off on either side. This is an unusual occurrence in a monitoring trend when the aerosol concentrations are higher during the rainy months (JJAS months - Fig. 3d). A similar pattern is observed in the columnar AOD values indicating higher aerosol loading during this period. On average, the change in the concentrations is 40–50 %. The unique spike during the rainy season is due to an increase in biomass burning rates, which corresponds to a rise in the number of hours when the 2-m temperature is below 10 °C and 15 °C (Fig. 3c), a threshold for household space heating demand. The percentage of hours under 15 °C is approximately 50 % compared to 30–40 % for the rest of the year and the percentage of hours under 20 °C is more 90–95 % compared to 70–80 % for the rest of the year. Most of the heating demand in the region is compensated via biomass burning.

The annual airshed average TROPOMI UVAI, shown in the table, indicates a 60 % increase in its residual value. A negative residual UVAI value suggests the presence of non-absorbing aerosols like sulfates, while a positive residual value indicates absorbing aerosols such as dust and smoke. The positive shift in values for 2023 compared to 2019 points to increased dust and smoke in the city, which may be due to more road dust from vehicle movement, increased construction activities, higher diesel combustion producing black carbon, and increased biomass burning generating organic carbon. The negative shift in 2020 likely reflects reduced vehicle activity during the COVID-19 lockdown and subsequent periods. Between 2019 and 2023, annual average PM<sub>2.5</sub> concentrations increased by 30 %.

A source apportionment study conducted by the Eastern Africa Global Environmental and Occupational Health (GEOHealth) Hub from Nov-2015 to Nov-2016, measured daily PM<sub>2.5</sub> concentrations of  $53.8 \pm 25.0 \mu\text{g}/\text{m}^3$  at one location in the city [38]; [39]. 90 % of the samples collected during this exercise exceeded the WHO guideline of  $5 \mu\text{g}/\text{m}^3$ . A similar monthly average trend, as shown in Fig. 4, was also observed in the samples collected at this station.

**Table 3**

Monthly and annual average PM<sub>2.5</sub> concentrations for the period of 2016–2024 measured at the US Embassy in Addis Ababa under the AirNow International program; annual airshed average of TROPOMI ultraviolet aerosol index (UVAI) for the period of 2019–2023; and monthly and annual airshed average of MODIS-MAIAC aerosol optical depth (AOD) for the period of 2019–2023.

Year	JAN	FEB	MAR	APR	MAY	JUN	JUL	AUG	SEP	OCT	NOV	DEC	Annual	UVAI
<b>PM<sub>2.5</sub> ambient monitoring data (µg/m<sup>3</sup>)</b>														
2016														<b>Annual</b>
2017	18.4	18.9	17.7	19.8	25.3	37.4	39.2	27.5	35.8	22.9	21.3	23.5	25.7	
2018	30.0	19.3	25.3	23.6	28.4	42.8	34.5	29.9	23.4	16.3	15.8	18.1	25.8	
2019	17.9	15.2	17.9	20.2	18.5	33.6		28.1	30.1	15.4	17.4	18.6	20.7	-0.99
2020	23.0	21.0	25.8	19.9	24.1	37.2	29.6	25.9	31.8	20.2	18.4	18.2	24.5	-1.28
2021	23.6	26.0	16.8	21.6	22.1	32.7	31.6	30.5	35.2	22.7	20.5	18.8	24.9	-1.00
2022	19.6	26.2	26.0	25.2	35.0	40.4	36.4	31.7	37.3	23.2	21.1	21.9	28.0	-0.26
2023	18.8	20.6	20.1	19.8	28.0	38.7	35.7	34.0	37.5	21.5	19.6	23.5	26.7	-0.40
2024	26.6	22.0	20.3	24.8	31.2	32.5								
<b>MODIS-MAIAC AOD</b>														
2019	0.18	0.25	0.26	0.24	0.12	0.48	0.39	0.35	0.37	0.17	0.22	0.11	0.18	
2020	0.17	0.21	0.35	0.23	0.23	0.36	0.42	0.42	0.34	0.18	0.15	0.15	0.18	
2021	0.21	0.21	0.21	0.26	0.17	0.30	0.37	0.34	0.32	0.15	0.17	0.15	0.19	
2022	0.10	0.20	0.25	0.31	0.25	0.42	0.37	0.36	0.21	0.13	0.11	0.13	0.16	
2023	0.16	0.21	0.28	0.20	0.19	0.34	0.39	0.27	0.34	0.15	0.11	0.18	0.17	

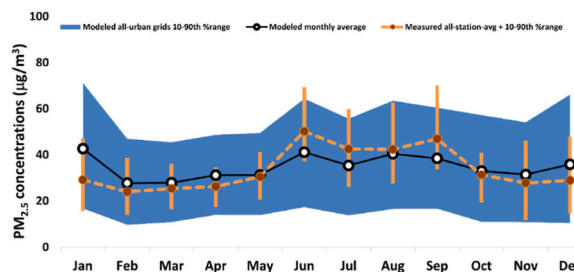


**Fig. 4.** Variation in the PM<sub>2.5</sub> concentrations among all the ambient monitoring stations (orange lines), modeled monthly average PM<sub>2.5</sub> concentrations from the WRF-CAMx system (black line), and variation in the PM<sub>2.5</sub> concentrations among all the urban grids in the airshed in a month (blue band).

### 3.3. Total emissions

The multi-pollutant emissions inventory summarized in Table 4 had major contributions from vehicle exhaust and dust resuspension from vehicle movement; residential and commercial activities like cooking, lighting, and baking; resuspension of dust from construction activities and erosion from quarries; open waste burning; and industrial biomass and fossil fuel combustion. In the main urban area, vehicle exhaust is the highest contributor with up to 29 % of total PM<sub>2.5</sub>, 16 % of PM<sub>10</sub>, 97 % of NO<sub>x</sub>, 71 % of SO<sub>2</sub> and 96 % of CO<sub>2</sub>. The transport sector is the primary contributor to SO<sub>2</sub>, NO<sub>x</sub>, and CO<sub>2</sub> emissions. The diesel-based heavy-duty and light-duty vehicles and passenger buses are responsible for 80 % of the total PM<sub>2.5</sub> emissions and on a fuel basis. With diesel sales at 6–7 times petrol sales and a higher emission rate associated with diesel exhaust, PM<sub>2.5</sub> emissions from diesel combustion is 95 %. While emissions from open waste burning and diesel generator sets are small at the airshed level, they are mostly concentrated in the core urban parts of the city. Due to the coarse nature of the dust, its contribution is higher in the total PM<sub>10</sub> emissions. Biomass burning in the domestic and industrial sectors dominates total CO and VOC emission rates. Open biomass fires were detected over in VIIRS satellite observations over the region and are an important emission source in Ethiopia. However, the fire instances had limited influence on GAAR. SO<sub>2</sub> emissions are expected to drop between 2018 and 2030, due to an expected improvement in the fuel quality reducing the average sulfur content in diesel from the current 500 ppm–50 ppm or less in 2030.

The emissions inventory is maintained in gridded CAMx model-ready format (Fig. 5a). The spatial distribution of emissions combines total emission calculations and multiple layers of GIS feeds for various sectors. For convenience, only PM<sub>2.5</sub> maps are presented in the figure. Monthly total emission maps and temporal profiles are included in the composite presentation in the supplementary materials. For the sectors with strong temporal profiles, the calculations were linked to the meteorological fields. For example, the heating energy demand was linked to the surface temperature with a threshold of 14 °C – lower the running mean, especially during the colder months and night times, higher the demand for heating and subsequently the emissions. The road dust emissions were modulated using the precipitation fields – for example, the grids and the hours with a threshold precipitation of 0.1 mm, the resuspended emissions were zeroed to avoid any overestimations, despite the active wet-deposition scheme in the CAMx model. This monthly and hourly modulation improved the temporal representation of the emissions.

In the absence of a published gridded emissions inventory representing GAAR at this spatial resolution, no direct or indirect comparisons were made with studies discussing an emissions inventory for the city. The final spatial disaggregation pattern of the total emissions is validated with a comparison of modeled and measured concentrations from the airshed. For this emissions inventory, no primary surveys were conducted for any of the sectors and all the analysis relied on available publications from official and unofficial sources. Overall, there is an average uncertainty of ±20–30 % in the total emissions. The emissions inventory and the spatial disaggregation procedures will be updated as and when new information is available for any or all the sectors.

Previous studies were limited in scope to make direct comparisons for all pollutants. Based on the available results from two studies, we summarized the overlaps and differences here. (a) C40 cities program report (C40report) presented, for the base year 2016, estimates of GHG emissions only, along with energy consumption rates and patterns. C40report showed total CO<sub>2</sub> emissions from the transport sector as 8.0 million tons, excluding non-CO<sub>2</sub> gas estimates, which is in the same ballpark as this study's estimate (8.6 million tons). A similar comparison is not possible for domestic and industrial sectors, because this study assumed "zero" CO<sub>2</sub> emission rate for

**Table 4**  
Modeled total emissions for the greater Addis Ababa airshed region.

tons/year	PM <sub>2.5</sub>	PM <sub>10</sub>	NO <sub>x</sub>	CO	VOC	SO <sub>2</sub>	CO <sub>2</sub>
All transport	7850	8050	120,100	94,200	10,750	4550	8,683,250
Residential	7300	7450	100	101,500	15,100	900	157,800
All industries	6650	7700	2950	47,000	13,700	850	92,250
All dust	3950	26,100	–	–	–	–	–
Open waste burning	850	900	–	4050	800	–	5400
Diesel generator sets	200	200	1250	3950	1750	50	120,000
Total	26,800	50,400	124,400	250,700	42,100	6,350	9,058,700

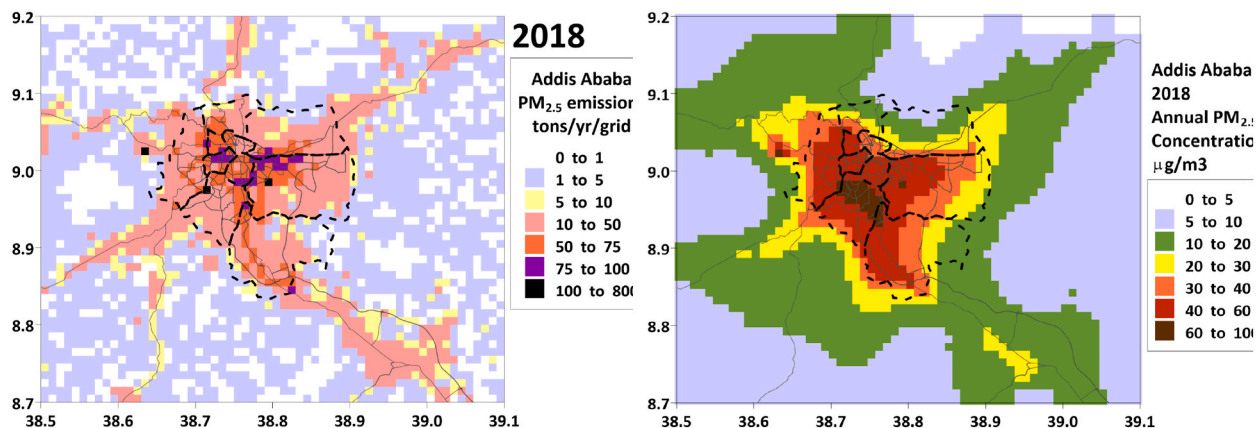


**Fig. 5.** (a) Estimated annual gridded PM<sub>2.5</sub> emissions for GAAR and (b) Modeled annual average PM<sub>2.5</sub> concentrations from WRF-CAMx modeling system.

renewable biomass fuel (anything wood). C40report did not present total or gridded emission estimates or modeled pollution estimates for the city or the airshed for other pollutants like PM, SO<sub>2</sub>, NO<sub>x</sub>, CO, and VOCs. (b) CSE's urban AQM guidance report (CSEreport) presented, for the base year 2002 and projections to 2014–15, estimates of total PM and NO<sub>x</sub> emissions from road transport only. CSEreport showed total PM and NO<sub>x</sub> emissions in 2014–15 from the transport sector as 3000 and 65,000 tons respectively and this study estimated double these numbers for 2018–19, which can be attributed to an increase in both the total number of registered vehicles and their usage between 2014 and 2018. The geographical sizes in the studies are also different, as this study includes the provinces in the immediate vicinity of Addis city with potential to contribute to the daily emission loads from vehicles not registered in the city. CSEreport also did not present total or gridded emission estimates or modeled pollution estimates for the city or the airshed for other sectors and other pollutants. While both the studies (C40report and CSEreport) presented an exponential increase in the total emissions of PM<sub>2.5</sub> and NO<sub>x</sub> from the transport sector, it is our understanding that the total emissions from the transport sector are likely to decrease due to an improvement in the vehicle technology of both the new vehicles and the imported secondhand vehicles from Japan and Europe. After 2024, assuming the average age of a secondhand vehicle is between 5 and 10 years, the new secondhand vehicles will have to be of Euro-3 or better technology, and thus improving the overall vehicle fleet quality and fleet average emission factor, thus reducing the total emissions. Similar improvements are not expected in the domestic and industrial sectors.

### 3.4. Modeled PM<sub>2.5</sub> concentrations, validation, and source apportionment

Estimated annual average PM<sub>2.5</sub> concentrations for GAAR from the WRF-CAMx modeling system are presented in Fig. 5b and monthly average concentration maps are presented in Fig. 6a. These concentrations include contributions of primary PM<sub>2.5</sub> emissions, secondary contributions from chemical conversion of SO<sub>2</sub> and NO<sub>x</sub> emissions in the form of sulfates and nitrate aerosols, and contributions from sources outside the airshed in the form of boundary conditions. The annual average concentration profile overlaps with the gridded population, road density, and urban-rural classification patterns of the city. The peaks during the winter and rainy months overlap with the months with the highest share of hours with low 2m-temperatures, low wind speeds, and low mixing layer heights (Fig. 3).

The WRF-CAMx modeling system, coupled with the gridded emissions inventory, effectively reproduces both the spatial and temporal variations observed in the available ambient monitoring data (Fig. 4). This validates the baseline confidence in the estimated emission totals and spatial distribution patterns in the GAAR inventory. The blue band represents the variation in concentrations across all 600 urban grids each month. The solid black line shows the modeled monthly average concentration, while the dashed orange line indicates the measured monthly average concentration and its intra-month variation from monitoring stations (including regulatory and sensor data). Discrepancies arise from variations in the modeled meteorological fields, the modeled emissions inventory, and the locations of the monitoring stations. All the monitoring stations, reference-grade and low-cost sensors are in the northern sector of the city (Fig. 1b) which typically record lower concentrations compared to the city center and the southern sector with most of the industrial and commercial activities. Since the modeled data covers a larger area of the urban agglomeration, variations are evident when comparing concentration fields. Moving forward, the comparison should be expanded to include a more extensive monitoring network covering a broader range of representative locations. This will help refine the initial emissions inventory for GAAR. The qualitative and quantitative overlap between existing monitoring data and modeled concentrations can serve as a foundation for analyzing potential emission control strategies and their anticipated benefits, such as reductions in ambient concentrations, improvements in public health outcomes, and mitigations against environmental degradation costs.

The WRF-CAMx modeling system was used to estimate the contribution of different source blocks (Table 4). We employed the brute-force method for source apportionment, which involves running multiple simulations—one with all emissions and others with each sector's emissions removed. This approach estimates source contributions by comparing the all-sector emissions simulation with simulations excluding one sector at a time. For GAAR, six simulations were conducted: one with all emissions and five with each

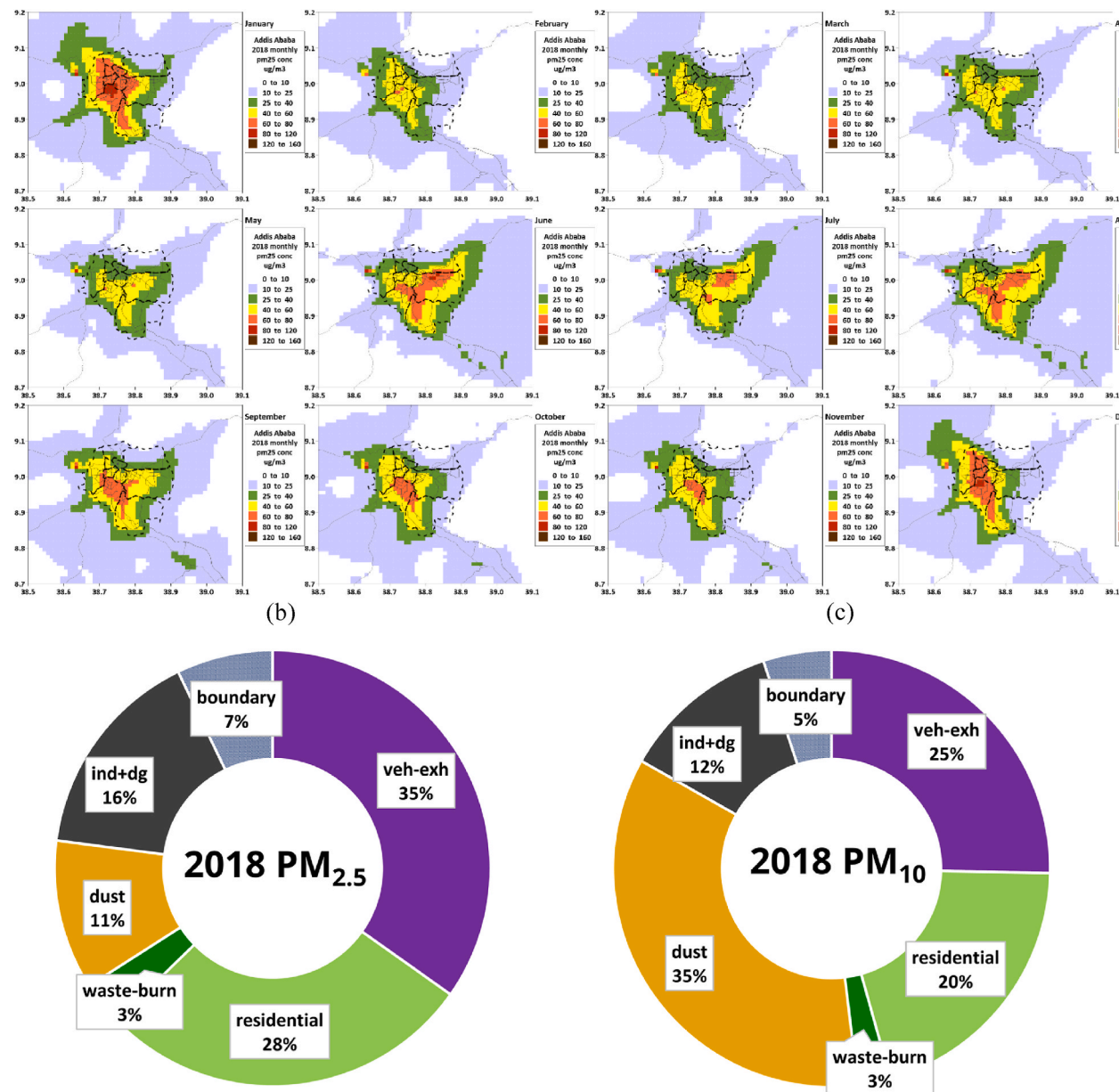


**Fig. 6.** (a) Modeled monthly average  $\text{PM}_{2.5}$  concentrations from the WRF-CAMx modeling system (b) Modeled source apportionment shares for  $\text{PM}_{2.5}$  annual average concentrations and (c) modeled source apportionment shares for annual average  $\text{PM}_{10}$  concentrations.

sector's emissions removed. The boundary conditions for the CAMx simulations are extracted from the global chemical transport model MOZART/CAM-chem (Table 1) to account for contribution of sources outside the airshed. These boundary conditions remain constant for all the simulations. The results presented in Fig. 6b–c represent only the grids within the district lines (Fig. 1a) and not the entire airshed. Modeled source contributions for GAAR reveal (a) annually,  $\text{PM}_{2.5}$  pollution is primarily from vehicle exhaust, biomass combustion, and dust, with vehicle exhaust consistently as the main source (b) dust significantly contributes to  $\text{PM}_{10}$  annually, particularly from resuspended road dust due to vehicle movement (c) biomass fuels, including wood, crop residue, cow dung, and charcoal, dominate non-transport sources, used widely for residential cooking, baking, and some rural space heating (d) Open waste burning and diesel generator sets make minor but noticeable contribution (e) the "boundary" indicates pollution transported from outside the airshed, influencing local pollution levels. The overall boundary contribution remains below 10 % throughout all months, suggesting a minor impact from sources outside the city airshed. This contribution tends to be higher during months with easterly winds. The source apportionment estimates by month are included in the supplementary. The peak  $\text{PM}_{2.5}$  season in the airshed (June to September months) corresponds to an increased use in biomass burning to support the space heating demand.

Similar findings were observed in the only source apportionment study, where samples were collected at a single station [39].

While these findings are based on data from a single location and may not be representative of the entire airshed, the higher presence of carbon components suggests significant contributions from biomass and diesel combustion, with additional contributions from crustal dust elements. Total carbon components contribution was 50 % more during June to September months, compared to the rest of the sampling period, along with a peak in the overall concentrations, again linking it to lower 2m-temperatures (Fig. 3c) and higher biomass combustion rates. The fraction of secondary sulfates, nitrates, and ammonium aerosols is small, indicating limited long-range contribution – conclusions consistent with the emissions-based modeling results (Fig. 6b). A summary comparison between the two approaches is included in a composite presentation in the supplementary.

#### 4. Way forward

This study presents the first open-access information baseline for GAAR, including model-ready emissions inventories, an application of a chemical transport model for generating pollution heatmaps, and source contribution estimates. To strengthen these results, a top-down chemical analysis-based study at multiple representative locations across the airshed is needed. This will enhance confidence in the findings and support long-term policy planning. Additionally, the modeling system could be expanded to enable short-term air quality forecasting. By simulating daily weather and pollution patterns for the next 3–5 days, this platform could provide timely pollution and health alerts to the public.

Addis Ababa's city council is advancing its first AQM plan (as of 2024), which highlights gaps in basic information, analytical work on ambient air quality monitoring, and weak institutional capacity. Recognizing the link between air pollution and public health, these initiatives underscore the importance of improving air quality for the well-being of urban residents. Some key components discussed in the preparation of an AQM plan for Addis Ababa and in other Ethiopian cities are: (a) Strengthening of institutional arrangements, environmental regulations, policy reforms, including new ambient air quality standards, industrial and tailpipe emission standards, governance structure, capacity building, and financial obligations; (b) Replication of the AQM plans in other Ethiopian cities following the example of Addis Ababa, to develop a national clean air plan with robust information baseline to guide, implement, and audit the emission control programs; (c) Expanding the ambient monitoring network using a combination of regulatory and sensor networks in a hybrid fashion, coupled with the emerging techniques to include satellite observations and other global model results; (d) Approving a national air quality index mechanism to initiate regular public awareness activities (e) Deepen the analytical skills at the environmental agencies in Addis Ababa (and Ethiopia) to establish capacity to routinely conduct consumption pattern surveys, emission inventories, air pollution modeling, source apportionment, and cost-benefit analysis of options; (f) Explore emission control options for sectors most using biomass (residential and industries) and vehicle exhaust, as these two are prioritized as major contributing sources to the ambient air pollution in Addis Ababa.

#### CRediT authorship contribution statement

**Sarath K. Guttikunda:** Writing – review & editing, Writing – original draft, Resources, Methodology, Investigation, Formal analysis, Data curation, Conceptualization. **Sai Krishna Dammalapati:** Writing – review & editing, Software, Resources, Investigation, Data curation. **Worku Tefera:** Writing – review & editing, Resources, Investigation, Data curation. **Jian Xie:** Writing – review & editing, Writing – original draft, Supervision, Resources, Investigation, Formal analysis, Conceptualization.

#### Data availability

All the data compiled for the emissions and pollution analysis, including a model-ready gridded emissions inventory covering the greater Addis Ababa airshed region; a composite presentation summaries of monitoring data, satellite retrievals, emission activities, emissions inventory and pollution modelling; and some supporting extracts from open GIS databases is included at <https://doi.org/10.5281/zenodo.12578908>. Updated MS-Excel based emissions and pollution modelling tools to conduct a capacity building training at the universities and public body forums is available @ <https://www.urbanemissions.info/tools>.

#### Funding statement

Authors acknowledge and thank the World Bank Group (Washington DC, USA) for supporting the initial phase (2019–20) of the analytical work.

#### Declaration of competing interest

The authors declare the following financial interests/personal relationships which may be considered as potential competing interests: Jian Xie reports financial support and administrative support were provided by The World Bank Group (Washington DC, USA). Other authors declare that they have no known competing financial interests or personal relationships that could have appeared to influence the work reported in this paper.

#### Acknowledgments

The analysis and conclusions presented herein are exclusively those of the authors and do not represent the supporting

organizations or the educational departments.

## References

- [1] D. Fowler, J.A. Pyle, M.A. Sutton, M.L. Williams, Global air quality, past present and future: an introduction, *Phil. Trans. Math. Phys. Eng. Sci.* 378 (2020) 20190323.
- [2] C.A. Miller, Fifty years of EPA science for air quality management and control, *Environ. Manag.* 67 (2021) 1017–1028.
- [3] D. Schwela, G. Haq, C. Huijzen, W. Han, H. Fabian, M. Ajero, *Urban Air Pollution in Asian Cities - Status, Challenges and Management*, Earthscan Publishers, London, UK, 2006.
- [4] D. Okure, S.K. Guttikunda, R. Sserunjogi, P. Adong, S.K. Dammalapati, D. Lsoto, P.P. Green, E. Bainomugisha, J. Xie, Integrated air quality information for Kampala: analysis of PM<sub>2.5</sub>, emission sources, modelled contributions, and institutional framework, *Environ. Sci.: Atmos* 5 (2025) 471–484.
- [5] R.M. Garland, K.E. Altieri, L. Dawidowski, L. Gallardo, A. Mbandi, N.Y. Rojas, N.d.E. Touré, Opinion: Strengthening Research in the Global South: Atmospheric Science Opportunities in South America and Africa, vol. 2023, EGU<sup>sphere</sup>, 2023, pp. 1–14.
- [6] A. Abera, J. Friberg, C. Isaxon, M. Jarrett, E. Malmqvist, C. Sjöström, T. Taj, A.M. Vargas, Air quality in Africa: public health implications, *Annu. Rev. Publ. Health* 42 (2021) 193–210.
- [7] E.A. Brakema, A. Tabyshova, R.M.J.J. van der Kleij, T. Sooronbaev, C. Lionis, M. Anastasaki, P.L. An, L.T. Nguyen, B. Kirenga, S. Walusimbi, M.J. Postma, N. H. Chavannes, J.F.M. van Boven, P. Le An, M. Anastasaki, A. Akylbekov, A. Barton, A. Bertsias, P.D.U. Binh, J.F.M. van Boven, E.A. Brakema, D. Burges, L. Cartwright, V.E. Chatzea, N.H. Chavannes, L. Cragg, T.N. Dang, I. Dautov, B. Emilo, I. Ferarrio, F.A. van Gemert, B. Hedrick, L.H.T.C. Hong, N. Hopkinson, E. Isaeva, R. Jones, C. de Jong, S. van Kampen, W. Kataigira, B. Kirenga, J. Kjærgaard, R.M.J.J. van der Kleij, J. Kocks, L.T.T. Lan, T.T.D. Linh, C. Lionis, K. X. Loan, M. Mademilov, A. McEwen, P. Musinguzi, R. Nantanda, G. Ndezei, S. Papadakis, H. Pinnock, J. Pooler, C.C. Poot, M.J. Postma, A. Poulsen, P. Powell, N. N. Quynh, S. Reventlow, D. Sifaki-Pistolla, S. Singh, T. Sooronbaev, J.C. de Sousa, J. Stout, M.S. Østergaard, A. Tabyshova, I. Tsiligianni, T.D. Tuan, J. Tumwine, L.T. Van, N.N. Vinh, S. Walusimbi, L. Warren, S. Williams, F.A.I.R.C. On behalf of the, The socioeconomic burden of chronic lung disease in low-resource settings across the globe – an observational FRESH AIR study, *Respir. Res.* 20 (2019) 291.
- [8] HEI-SoGA, State of Global Air (SOGA). A Special Report on Global Exposure to Air Pollution and its Health Impacts, Health Effects Institute, Boston, USA, 2024.
- [9] K.R. Smith, N. Bruce, K. Balakrishnan, H. Adair-Rohani, J. Balmes, Z. Chafe, M. Dherani, H.D. Hosgood, S. Mehta, D. Pope, E. Rehfuss, Millions dead: how do we know and what does it mean? Methods used in the comparative risk assessment of household air pollution, *Annu. Rev. Publ. Health* 35 (2014) 185–206.
- [10] H. Wipfli, A. Kumie, L. Atuyambe, O. Ouguge, E. Rugigana, K. Zacharias, B. Simane, J. Samet, K. Berhane, The GEOHealth hub for Eastern Africa: contributions and lessons learned, *GeoHealth* 5 (2021) e2021GH000406.
- [11] A.B. Shiferaw, A. Kumie, W. Tefera, The spatial and temporal variation of fine particulate matter pollution in Ethiopia: data from the atmospheric composition analysis group (1998–2019), *PLoS One* 18 (2023) e0283457.
- [12] P.D.M.C. Katoto, L. Byamungu, A.S. Brand, J. Mokaya, H. Strijdom, N. Goswami, P. De Boever, T.S. Nawrot, B. Nemery, Ambient air pollution and health in Sub-Saharan Africa: current evidence, perspectives and a call to action, *Environ. Res.* 173 (2019) 174–188.
- [13] S. Keita, C. Liousse, E.M. Assamoi, T. Doumbia, E.T. N'Datchoh, S. Gnamien, N. Elguindi, C. Granier, V. Yoboué, African anthropogenic emissions inventory for gases and particles from 1990 to 2015, *Earth Syst. Sci. Data* 13 (2021) 3691–3705.
- [14] C. Liousse, E. Assamoi, P. Criqui, C. Granier, R. Rosset, Explosive growth in African combustion emissions from 2005 to 2030, *Environ. Res. Lett.* 9 (2014) 035003.
- [15] E.P. Petkova, D.W. Jack, N.H. Volavka-Close, P.L. Kinney, Particulate matter pollution in African cities, *Air Qual. Atmos. Health* 6 (2013) 603–614.
- [16] A. Singh, W.R. Avis, F.D. Pope, Visibility as a proxy for air quality in East Africa, *Environ. Res. Lett.* 15 (2020) 084002.
- [17] S.K. Guttikunda, N. Kalladath, V. Tejaswi, R. Goel, Fuel station survey (FuSS) to profile In-Use vehicle characteristics, SIM-air Working Papers #2025-56, 2025. <https://www.urbanemissions.info>.
- [18] D. Guta, H. Zerriffi, J. Baumgartner, A. Jain, S. Mani, D. Jack, E. Carter, G. Shen, J. Orgill-Meyer, J. Rosenthal, K. Dickinson, R. Bailis, Y. Masuda, Moving beyond clean cooking energy adoption: using Indian ACCESS panel data to understand solid fuel suspension, *Energy Policy* 184 (2024) 113908.
- [19] D. Fowler, P. Brimblecombe, J. Burrows, M.R. Heal, P. Grennfelt, D.S. Stevenson, A. Jowett, E. Nemitz, M. Coyle, X. Liu, Y. Chang, G.W. Fuller, M.A. Sutton, Z. Klmont, M.H. Unsworth, M. Vieno, A chronology of global air quality, *Phil. Trans. Math. Phys. Eng. Sci.* 378 (2020) 20190314.
- [20] GAINS, Greenhouse Gas and Air Pollution Interactions and Synergies (GAINS) by International Institute of Applied Systems Analysis (IIASA), 2024. Laxenburg, Austria, <https://iiasa.ac.at/models-tools-data/gains>.
- [21] S.K. Guttikunda, K.A. Nishadh, P. Jawahar, Air pollution knowledge assessments (APnA) for 20 Indian cities, *Urban Clim.* 27 (2019) 124–141.
- [22] UEinfo, Air pollution knowledge assessments (APnA) city program covering 50 airsheds and 60 cities in India. <https://www.urbanemissions.info>, 2024.
- [23] USEPA, AP-42: Compilation of Air Emissions Factors -, US-EPA, Washington DC, USA, 2022. <https://www.epa.gov/air-emissions-factors-and-quantification/ap-42-compilation-air-emissions-factors>.
- [24] J. Xie, W. Jia, L. Croitoru, S.K. Guttikunda, J. Grutter, Safe to Breathe Analyses and Recommendations for Improving Ambient Air Quality Management in Ethiopia, The World Bank, Washington DC, USA, 2021.
- [25] L. Kebede, G.S. Tulu, R.T. Lisinge, Diesel-fueled public transport vehicles and air pollution in addis Ababa, Ethiopia: effects of vehicle size, age and kilometers travelled, *Atmos. Environ.* X 13 (2022) 100144.
- [26] J. Grutter, Steering Towards Cleaner Air : Measures to Mitigate Transport Air Pollution in Addis Ababa, World Bank, Washington, DC, 2021.
- [27] T. Gebre, Assessment of CO<sub>2</sub> emission level in urban transport of Mekelle City, Ethiopia, *Ethiopian. J. Environ. Stud. Manag.* 9 (2016).
- [28] S. Neway, R.B. Nallamothu, S.K. Nallamothu, A.K. Nallamothu, Investigation on pollution caused by gasoline and diesel fuelled vehicles, *Int. J. Eng. Trends Technol.* 36 (2016) 376–381.
- [29] N.E. Benti, G.S. Gurmessa, T. Argaw, A.B. Aneseyee, S. Gunta, G.B. Kassahun, G.S. Aga, A.A. Asfaw, The current status, challenges and prospects of using biomass energy in Ethiopia, *Biotechnol. Biofuels* 14 (2021) 209.
- [30] A. Tolassa, Bioenergy potential from crop residue biomass resources in Ethiopia, *Heliyon* 9 (2023) e13572.
- [31] M.A.H. Mondal, E. Bryan, C. Ringler, D. Mekonnen, M. Rosegrant, Ethiopian energy status and demand scenarios: prospects to improve energy efficiency and mitigate GHG emissions, *Energy* 149 (2018) 161–172.
- [32] B. Firdissa, S. Degefa, E. Mulugeta, D. Sithole, Ethiopian cement plants: examining emissions and their impact on community well-being, preprints, 2024. Preprints, <https://www.preprints.org/manuscript/202401.1315/v1>.
- [33] G. Tesema, E. Worrell, Energy efficiency improvement potentials for the cement industry in Ethiopia, *Energy* 93 (2015) 2042–2052.
- [34] T.W. Bulto, Impact of open burning refuse on air quality: in the case of “Hidar Sitaten” at Addis Ababa, Ethiopia, *Environ. Health Insights* 14 (2020) 1178630220943204.
- [35] Y. Fitaw, B. Zenebre, Assessment of the landfill situation of Addis Ababa city administration, *Environ. J. Health. Sci.* 13 (2003).
- [36] D. Shewatake, B. Tenaw, A. Yemiru, G. Belete, T. Tadesse, T. Tolla, Characteristics of sand at major quarrying areas around Addis Ababa, *Adv. Civ. Eng.* 2022 (2022) 3198879.
- [37] H. Worku, Environmental and socioeconomic impacts of cobblestone quarries in Addis Ababa and implication for resource use efficiency, environmental quality, and sustainability of land after-use, *Environ. Qual. Manag.* 27 (2017) 41–61.
- [38] A. Kumie, A. Worku, Z. Tazu, W. Tefera, A. Asfaw, G. Boja, M. Mekashu, D. Siraw, S. Tefera, K. Zacharias, J. Patz, J. Samet, K. Berhane, Fine particulate pollution concentration in Addis Ababa exceeds the WHO guideline value: results of 3 years of continuous monitoring and health impact assessment, *Environ. Epidemiol.* 5 (2021) e155.
- [39] W. Tefera, A. Kumie, K. Berhane, F. Gilliland, A. Lai, P. Sricharoenvech, J. Patz, J. Samet, J.J. Schauer, Source apportionment of fine organic particulate matter (PM<sub>2.5</sub>) in central Addis Ababa, Ethiopia, *Int. J. Environ. Res. Publ. Health* 18 (2021) 11608.